

# Loading Phase Angle Effect on Multiaxial Behaviour of 30CrNiMo8HH

M. Noban<sup>1</sup>, H. Jahed<sup>1</sup> and A. Ince<sup>1</sup>

<sup>1</sup>Fatigue & Stress Analysis Laboratory, Mechanical & Mechatronics Engineering Department, University of Waterloo, 200 University Ave W, Waterloo, ON, CANADA; TEL: +1 519 888 4567 x37826; E-mail: [hjahedmo@uwaterloo.ca](mailto:hjahedmo@uwaterloo.ca)

**ABSTRACT.** *Nonproportional or out-of-phase loading refers to stress/strain history that result in rotation of the principal axes of stress/strain during a cyclic loading. The effect of such loading on 30CrNiMo8HH steel is discussed here. It is shown that material's life is significantly reduced when load phase angle is increased. An energy approach is utilized to correlate the fatigue life results obtained from proportional and nonproportional loading experiments. Through a proposed life estimation model based on a modified energy fatigue damage parameter, a good agreement is established between experimental and estimated fatigue results.*

## INTRODUCTION

Experiments on different materials have shown that nonproportional multiaxial loading decreases the fatigue life significantly and that the low cycle nonproportional loading is more damaging than proportional loading [1-3]. In a nonproportional loading the planes of maximum shear strain/stress rotate and thus initiate plastic deformation along several different slip systems. Such slip systems activation in a nonproportional loading is more in comparison to proportional loading. More activated slip systems results in more damage in nonproportional loading.

The high strength 30CrNiMo8HH steel is widely used in applications subjected to multiaxial and in particular nonproportional loading. It is therefore important to examine its behaviour dependency on load path in search for a suitable fatigue model. Gerhard et al [4] reported a set of experiments on the fatigue of thick-walled plain and cross-bored pipes made from high CrNi steels alloy under pulsating internal pressure. Influence of multiaxial loading on the fatigue life of chrome nickel based metals has also been studied under stress control conditions by J. Hug and H. Zenner [5]. Putter et al [6] investigated fatigue life of 30CrNiMo8 steel under combined bending and torsion for notched specimens. Lagoda and Macha [7-8] calculated fatigue life of a chrome nickel alloy steel based on three different criteria of multiaxial fatigue and under stress control loading. They employed Palmgren-

Miner hypothesis to calculate fatigue under random loading conditions. Ahmadi and Zenner [9] represented a model to simulate the damage progress based on the growth of micro-cracks under the influence of cyclic loading for steel alloys including 30CrNiMo8. Sonsino and Grubisic [10] considered 30CrNiMo8 multiaxial fatigue using cylindrical specimens.

In this paper the nonproportionality of load effect on multiaxial behaviour of 30CrNiMo8HH steel is studied. A set of biaxial tests including strain controlled proportional and nonproportional loads were performed. Experiments of in-phase and 90-degree-out of phase loading have been used to characterize and model the fatigue behaviour of 30CrNiMo8HH steel alloy under different load paths. It has been observed that proportional loading and 90-degree-out of phase loading are representing lower and upper damaging limit for predicting fatigue life of this metal under different load paths. It was observed that the 90 degree's out-of-phase loading has more damaging effect in comparison to proportional loading which is in agreement with the results of Sonsino and Grubisic [10]. An energy parameter [11 & 12] has been modified to account for nonproportionality effect of the material and is used for correlation of results. Life estimated by the proposed model is compared to experimental life. Agreements of the results are good.

## Material and Tests

All tests were conducted in strain control mode on tubular specimen (Figure 1) machined from an actual component made of 30CrNiMo8HH.

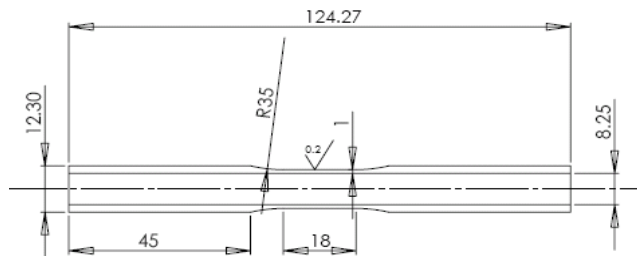


Figure 1: Specimen geometry. All dimensions in (mm) except for surface roughness ( $\mu\text{m}$ )

The gross properties of the material were obtained by optical microscopy and image analysis conducted on virgin tubular samples. The specimen was sectioned and cold-mounted in epoxy resin. The mounted specimens were then ground and polished to a mirror-finish using 1200 and 4000 grit SiC paper; followed by 3, 1 and  $\frac{1}{4}$   $\mu\text{m}$  diamond paste. The as-received sample was viewed through the thickness of the tube. After standard

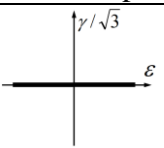
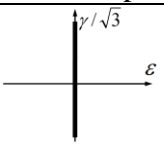
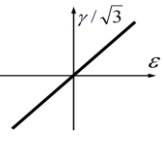
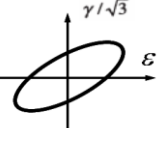
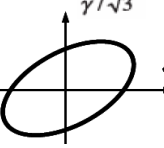
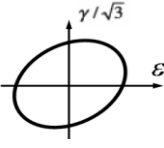
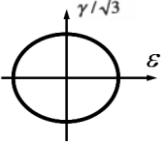
metallographic preparation and etching with a 2% Nital solution, a fine lath martensite structure was revealed for the 30CrNiMo8HH alloy steel studied.

Vickers hardness measurements were conducted on the as-received material using a micro-hardness testing machine. The specimen was ground and polished to a mirror-finished as described above. To determine the homogeneity of the tube properties, hardness measurements were taken through the thickness of the tube at the 0, 3, 6, and 9 o'clock tube positions at regular intervals of 110 $\mu$ m and compared. No variation in hardness was measured through the thickness of the sample or at the different tube locations. The overall mean Vickers hardness number (VHN) of the undeformed alloy was found to be 331.2.

Tensile tests were performed according to ASTM Standard E8M-04. A total of four tests under room temperature were done on servo hydraulic test machine. The results of the tensile tests show an average yield strength of 870 MPa, ultimate strength of 1025 MPa, modulus of elasticity of 200 GPa, percentage elongation of 30%, area reduction close to 63%, and Romberg-Osgood parameters:  $K$  of 1240 MPa, and  $n$  of 0.061.

Cyclic axial and biaxial tests are performed at room temperature on a servo hydraulic tension-torsion machine based on ASTM-E606 and ASTM-E2207, respectively. Table 1 represents the load paths considered in the experiments.

Table 1: Different applied load paths

Load path name	Load shape	Load path name	Load shape
In-phase: Axial loading		In-phase: Shear loading	
In-phase strain		30° Out of phase	
45° Out of phase		60° Out of phase	
90° Out of phase			

Test results are summarized in Table 2.

Table 2: Summary of fatigue test results

SP	Load shape	Axial strain amplitude (mm/mm)	Shear strain amplitude (Radians)	Life	SP	Load shape	Axial strain amplitude (mm/mm)	Shear strain amplitude (Radians)	Life
1	axial	0.00715	0	1649	1	in phase	0.003451	0.003226	4493
2	axial	0.00706	0	1221	2	in phase	0.003451	0.003228	3903
3	axial	0.00461	0	3064	3	in phase	0.004228	0.004776	1885
4	axial	0.00508	0	2200	4	in phase	0.003676	0.004174	2699
5	axial	0.00401	0	12700	5	30° out of phase	0.003496	0.006568	1346
6	axial	0.00335	0	26302	6	30° out of phase	0.003493	0.006554	2240
7	axial	0.00418	0	11484	7	30° out of phase	0.003474	0.006594	1885
8	axial	0.0097	0	500	8	45° out of phase	0.003483	0.006828	1171
9	shear	0	0.005306	1414	9	45° out of phase	0.003468	0.00662	1645
10	shear	0	0.00539	1833	10	60° out of phase	0.003486	0.006592	1425
11	shear	0	0.00539	2341	11	60° out of phase	0.003495	0.006667	1414
12	shear	0	0.003978	5200	12	90° out of phase	0.003557	0.006782	1384
13	shear	0	0.004029	5500	13	90° out of phase	0.003495	0.006766	1264
14	shear	0	0.006962	793	14	90° out of phase	0.003148	0.006072	1777
15	shear	0	0.006893	1100	15	90° out of phase	0.002939	0.005602	1932

Fractography of the fatigue specimens tested under pure torsion and nonproportional (NP) loading conditions were performed using SEM. Visual examination of the fatigue samples reveals that crack initiation occurs at the outer surfaces of the tube. Comparing specimens that were under pure torsion and NP loading conditions; cracks were found to initiate and grow along the gauge length of the tube before branching out perpendicularly for the former, whilst cracking occurs perpendicularly for the latter.

Figure 2 shows the typical fracture surfaces of the NP fatigue specimens. Much of the surface is damaged due to repeated rubbing of the two faces during fatigue testing. Closer examination of the damaged surface reveals that some micro-cracking or porosity is present in the fatigue samples. These cracks were not observed in the undeformed sample and were generated during fatigue testing. They are likely to have initiated at second-phase inclusions present within the material before propagating and connecting with other neighboring voids. Figure 3 show the fracture surface of a sample which was tested under pure torsion conditions. The presence of micro cracks originating from outer surface of the tube specimen can be seen in Figure 3. Figure 4a) shows a micro crack initiated from where an oxide impurity is present. Throughout the surface and within crevices of the micro cracks, small second-phase particles are present (Figure 4b). Qualitative EDX analysis

found that they are Mn-rich sulphites or Fe-Cr-Ni-rich intermetallics. These observations are in agreement with the findings of Yang and Saxena [13], which suggest that fatigue cracks initiate from slip bands and accumulate at discontinuities near the surface of the specimen.

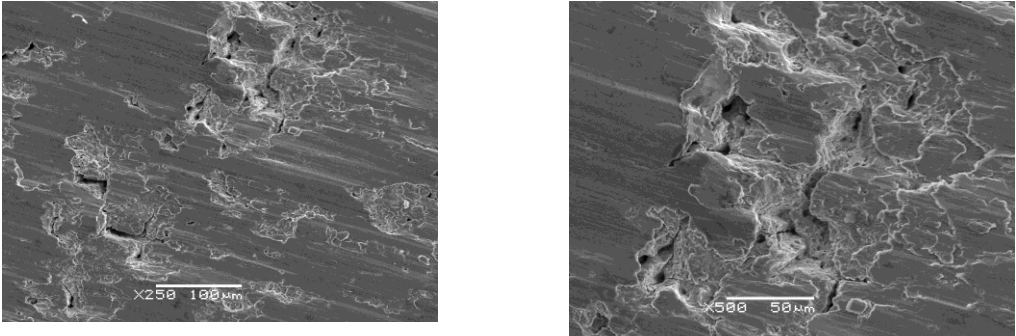


Figure 2: Cracking and porosity present below the damaged fracture surface of specimen.

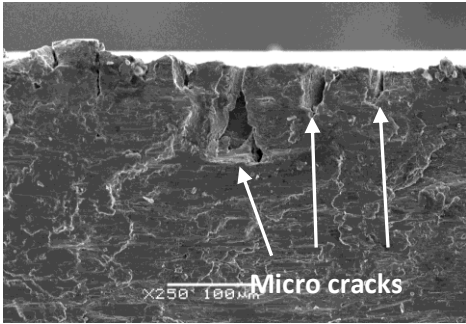


Figure 3: SEM images of the outer surface of torsion sample

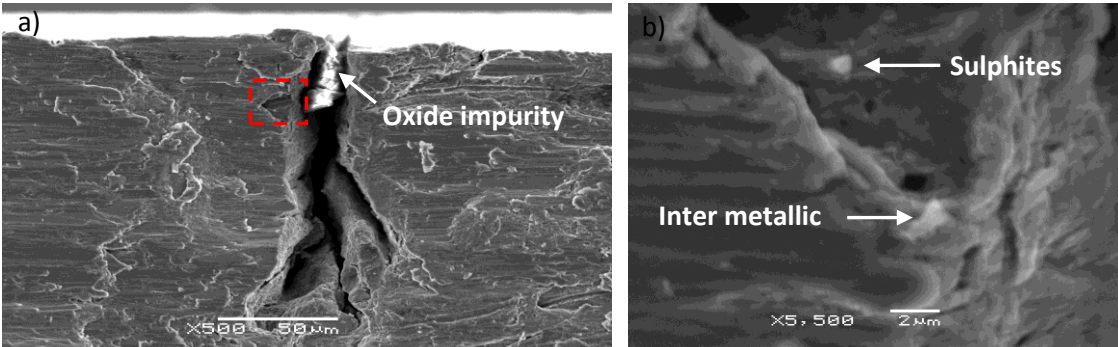


Figure 4: a) micro crack originating from a large oxide impurity, and b) higher-resolution image of region highlighted in a) showing the presences of sulphites and inter metallic.

## FATIGUE CORRELATION

An energy damage parameter based on plastic energy dissipated and positive elastic energy recovered in each cycle is considered for correlation of the fatigue data.

Correlation of the results measured from experimental results as fatigue damage parameter is shown in Figure 5. Experiments show that a power law function is suitable for relating damage parameter,  $D_p$  to fatigue life (Eq.1):

$$D_p = f(N_{f_p}) = m (N_{f_p})^n \quad (1)$$

The two constants “ $m$ ” and “ $n$ ” are dependent on material and the damage parameter  $D_p$ . Least square fitting method can be used to best fit the curve with fatigue data points of proportional fatigue tests to obtain  $m=1418$  and  $n=-0.6747$ . Life estimated by equation (1) is compared to experimental results and are shown in Figure 6. While data for proportional loading agrees well, as expected, data for nonproportional loadings are not in an acceptable range. Clearly, there is a need to include nonproportionality effect into the fatigue model.

## PHASE ANGLE EFFECT MODIFICATION

There are two parts in this modification. One is material related and the other is loading path, i.e., phase angle, related. Materials have shown different properties under nonproportional loadings. An example of such properties is the additional hardening. Some materials, such as SS304, have shown significant additional hardening whereas some other materials, such as 1045 steel, have shown next to none. Here, to account for nonproportionality effect, a factor is being introduced which is the product of material and load path related properties. The part that has to do with the material properties is termed nonproportionality sensitivity factor  $\alpha$ . The part that has to do with the load history is termed phase angle factor  $\psi$ . The damage parameter introduced earlier may now be modified and related to life by:

$$D_{NP} = D_p(1 + \alpha\psi) \text{ and } N_{f_{NP}} = \left[ \frac{D_{NP}}{m} \right]^{\frac{1}{n}} = \left[ \frac{D_p(1 + \alpha\psi)}{m} \right]^{\frac{1}{n}} \quad (2)$$

The method of minimum circumscribed ellipse in strain space has been employed for determining load path effect in fatigue life calculation. The phase angle factor is defined as the ratio of the minor axis to major axis of the minimum circumscribed ellipse mapped onto strain load path. Also,  $\alpha$  the nonproportionality sensitivity constant can be determined by matching fatigue tests results of 90 degree's out-of-phase loading with fatigue results of in-phase loading fatigue curve. These two loading represent two extremes of loading that

have shown minimum and maximum lives. By knowing the values for  $N_{f_{90}}$ ,  $D_p$  and  $\psi$  for the out-of-phase 90 degree's loadings tests and fatigue curve for proportional loading,  $\alpha$  can be found using the least square method. For energy damage parameter employed here  $\alpha=0.9$ .

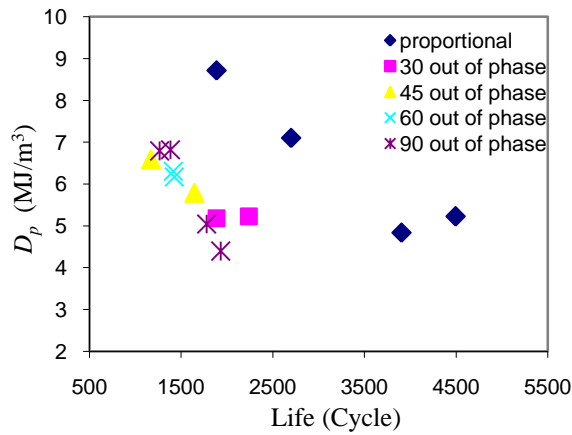


Figure 5: Correlation of the fatigue results.

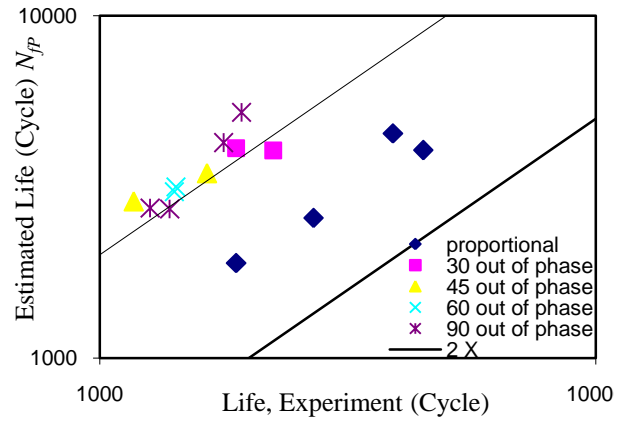


Figure 6: Estimated vs. experimental life.

Figure 7 show damage-life correlation after applying the modified damage parameter (Eq. 2). There is a much better correlation between the modified damage parameter and fatigue data. Using the same life parameters,  $m$  and  $n$ , obtained for the in-phase case, the fatigue life is estimated. The results are depicted in Figure 8.

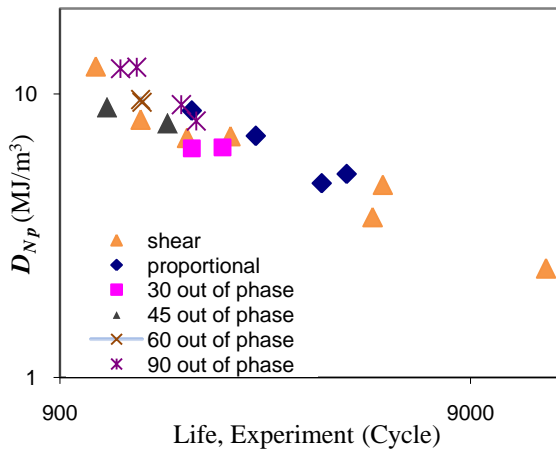


Figure 7: life correlation before and after applying nonproportionality factor.

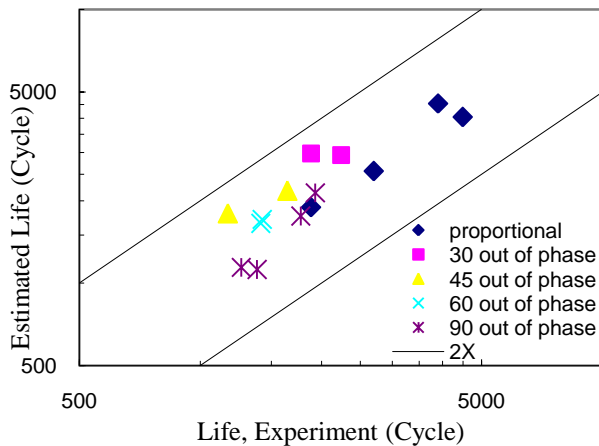


Figure 8: Estimated vs. experimental life using the modified fatigue damage parameter.



## CONCLUSIONS

The behaviour of 30CrNiMo8HH under nonproportional loading has been studied extensively. Based on experimental results and modeling discussed in this paper, following general conclusions are drawn:

- 1- While many non propagating micro cracks are forming at the outer surface soon after application of cyclic torsion, internal cracks due to second-phase intermetallic and impurities are also observed.
- 2- The material shows insignificant additional hardening when under nonproportional loading. However, the life is significantly reduced as the loading phase angle increased showing a strong material sensitivity to loading path.
- 3- An energy based fatigue damage parameter that incorporates the loading phase angle into account is proposed. It has been shown that the proposed parameter correlates the experimental results very well. Using the proposed fatigue-life model, lives at different loading paths were calculated and compared to experimental results. A good agreement exists between estimated and actual life.

## ACKNOWLEDGEMENT

Authors would like to acknowledge the financial support of the Natural Sciences and Engineering Research Council (NSERC) of Canada. Dr S. Winkler's help with the metallographic studies is greatly appreciated.

## REFERENCES

1. Chen X., Gao Q., and Sun F., (1996) *J Fatig Frac Eng Mater Struct* **19** (7), 839-854.
2. Chen X., Gao Q. and Sun X.-F., (1994) *Int. J. Fatigue* **16**, 211-215.
3. Socie D. and Marquis G., (1999) *Multi-axial fatigue*, SAE International.
4. Gerhard V., Diethelm L., and Gerhard M., (1992) *Chem. Eng. Technol.* **15**, 300-312.
5. Hug J., Zenner H., (1998), In: *Cycle fatigue and elasto-plastic behaviour of materials*, Kyong-Tschong Rie, Pedro D. Portella, Elsevier, 217-230.
6. Putter Y., Zenner H., (2000), In: *Multi-axial fatigue and deformation: testing and prediction*, Sreeramesh Kalluri, Peter J. Bonacuse, 157-172.
7. Lagoda T., Macha E., (1995) *Materials Science* **31**, 23-31.
8. Lagoda T., Macha E., (1994) *Fatigue Fract. Engng Mater. Struct.* **17**(11), 1307-1318.
9. Ahmadi A., Zenner H., (2006) *Int. J. of Fatigue* **28**(9), 954-962.
10. Sensino C., Gubisic V., (1985) *ASTM, STP 853, Multiaxial Fatigue*, 586-605.
11. Jahed H., Varvani A., Noban M., Khalaji I. (2007) *Int. J. Fatigue* **29**(4), 647-655.
12. Jahed H., Varvani A., (2006) *Int. J. Fatigue* **28**, pp 467-473.
13. F. Yang and A Saxena, (2000), *Proc. Instn. Mech. Engrs.* 214, Part C, 1151-1161.